Quasiperiodically kicked quantum systems

P. W. Milonni, J. R. Ackerhalt, and M. E. Goggin
Theoretical Division, Los Alamos National Laboratory, Los Alamos, New Mexico 87545
(Received 11 August 1986)

We consider a two-state system kicked quasiperiodically by an external force. When the two kicking frequencies assumed for the force are incommensurate, there can be quantum chaos in the sense that (a) the autocorrelation function of the state vector decays, (b) the power spectrum of the state vector is broadband, and (c) the motion on the Bloch sphere is ergodic. The time evolution of the state vector is nevertheless dynamically stable in the sense that memory of the initial state is retained. We also consider briefly the kicked quantum rotator and find, in agreement with Shepelyansky [Physica **8D**, 208 (1983)], that the quantum localization effect is greatly weakened by the presence of two incommensurate driving frequencies.

I. INTRODUCTION

The question of how classical chaos might manifest itself in quantum mechanics is an intriguing one. In systems with external driving forces there are some particularly interesting questions about diffusion in phase space and energy deposition; early numerical experiments of Casati *et al.*[1] have provided the impetus for much of the work in the field. These authors considered first the classical problem of a kicked rotator, which is described by the so-called standard map, and found that in a chaotic regime the angular momentum (P_θ) performs an essentially random walk with the energy (P_θ^2) growing linearly with time on average. When the same system was treated quantum mechanically, however, it was found that this diffusive energy growth is greatly suppressed.

This suppression of the classical diffusive behavior associated with chaotic time evolution was related by Grempel *et al.*[2] to the Anderson localization of a (quantum) particle in a one-dimensional lattice with random site energies. The random diagonal terms of the tight-binding model correspond in the periodically kicked quantum system to a pseudorandom sequence, with the lattice points of the tight-binding model corresponding to the integer values of quantized angular momentum in the rotator. The suppression of diffusion in the kicked quantum system is thus fully analogous to the localization in configuration space of an electron in a one-dimensional random lattice.

The localization analogy certainly suggests that the time evolution of driven quantum systems can be more orderly than the corresponding classical evolution. However, it does not necessarily mean that some classical notions of chaos are generally impossible in quantum mechanics. We consider here quantum systems driven *quasiperiodically*. In this case there are reasons to expect localization to be greatly weakened, as discussed below. We begin in Sec. II with a quantum map for a quasiperiodically kicked two-state system, and reach conclusions in agreement with Pomeau *et al.*[3] In particular, the autocorrelation function of the state vector is found to decay strongly when the Rabi frequency is large. We also present evidence that the motion on the Bloch sphere is ergodic, and give an intuitive explanation for the appearance of chaos. In Sec. III we return to the problem of the kicked quantum rotator, and present numerical evidence for diffusive energy growth when the rotator is kicked quasiperiodically. We argue that some aspects of deterministically chaotic behavior may be a general feature of quasiperiodically driven quantum systems.

II. THE TWO-STATE SYSTEM

Consider the general problem of a quantum system described by the Hamiltonian

$$H = H_0 + A(x)F(t)\sum_{-\infty}^{\infty}\delta(t/T - n)\ . \tag{2.1}$$

Let $|\Psi(k)\rangle$ be the state vector just before the kth δ-function impulse. Just after the kth impulse the state vector is $\exp[-iA(x)F(kT)T/\hbar]\,|\Psi(k)\rangle$, and between impulses the evolution of the state vector is governed by the operator $\exp(-iH_0t/\hbar)$. Thus

$$|\Psi(k+1)\rangle = e^{-iH_0T/\hbar}e^{-iA(x)F(kT)T/\hbar}\,|\Psi(k)\rangle\ . \tag{2.2}$$

Writing

$$|\Psi(k)\rangle = \sum_m a_m(k)\,|\psi_m\rangle\ , \tag{2.3}$$

where $H_0\,|\psi_m\rangle = E_m\,|\psi_m\rangle$, we obtain from (2.2) the quantum map

$$a_n(k+1) = \sum_m V_{nm}(k)a_m(k)\ , \tag{2.4a}$$

where

$$V_{nm}(k) \equiv \langle\psi_n|\,e^{-iA(x)F(kT)T/\hbar}\,|\psi_m\rangle e^{-iE_nT/\hbar}\ . \tag{2.4b}$$

In the case $F(t)=$const, V_{nm} is independent of k and we have a periodically kicked quantum system of the type considered by Casati *et al.*[1]

The case of a kicked two-state "atom" is particularly simple. In this case the unperturbed Hamiltonian $H_0=(\hbar\omega_0/2)\sigma_z$, where σ_z is a Pauli spin operator and ω_0 is the transition frequency. For the perturbation we take $A(x)=-\mu E\sigma_x$. In the example of a two-state atom in an

electric field, μ is the transition dipole matrix element and E the amplitude of the applied field, and a Rabi frequency is defined as $\Omega=\mu E/\hbar$. For this perturbation we have

$$e^{-iA(x)F(kT)T/\hbar}=e^{i\Omega F(kT)T\sigma_x}$$

$$=\cos[\Omega(k)T]+i\sigma_x\sin[\Omega(k)T]\ , \quad (2.5)$$

with $\Omega(k)\equiv\Omega F(kT)$, and the matrix elements V_{nm} are easily evaluated. Defining $c_n(k)\equiv a_n(k)e^{ikE_nT/\hbar}$, $n=1$ and 2, we may write (2.4) in the form

$$c_1(k+1)=\cos[\Omega(k)T]c_1(k)$$

$$+i\sin[\Omega(k)T]e^{-ik\omega_0T}c_2(k)\ , \quad (2.6a)$$

$$c_2(k+1)=i\sin[\Omega(k)T]e^{ik\omega_0T}c_1(k)$$

$$+\cos[\Omega(k)T]c_2(k)\ . \quad (2.6b)$$

Consider first the case of periodic kicking with $\Omega(k)\to\Omega$ independent of k. In Fig. 1 we plot the upper-state probability $|c_2(k)|^2$ versus the impulse number k for $\omega_0T=2\pi$ and $\Omega T=0.60$. [In each case we start with the initial condition $c_1(0)=1$ and $c_2(0)=0$.] It is interesting to compare such results with the solution of the Schrödinger equation for a two-state atom in a field $E_0\cos(\omega t)$. In Bloch form these equations are[4]

$$\dot{x}=-\omega_0 y\ , \quad (2.7a)$$

$$\dot{y}=\omega_0 x+\bar{\Omega}z\cos(\omega t)\ , \quad (2.7b)$$

$$\dot{z}=-\bar{\Omega}y\cos(\omega t)\ , \quad (2.7c)$$

where $\bar{\Omega}=\mu E_0/\hbar$. The atom is driven most strongly when $\omega\cong\omega_0$; driving frequencies ω far removed from resonance do not have much of an effect by comparison. Therefore we can replace $\cos(\omega t)$ in (2.7) by

$$\tfrac{1}{2}\sum_{-\infty}^{\infty}e^{in\omega t}=\tfrac{1}{2}\sum_{-\infty}^{\infty}e^{2\pi int/T}=\tfrac{1}{2}\sum_{-\infty}^{\infty}\delta(t/T-n)\ , \quad (2.8)$$

where $T=2\pi/\omega$, and we expect the mapping (2.6) to approximate well the solution of the Bloch equations whenever $\omega\cong\omega_0$ and $\bar{\Omega}=2\Omega$.

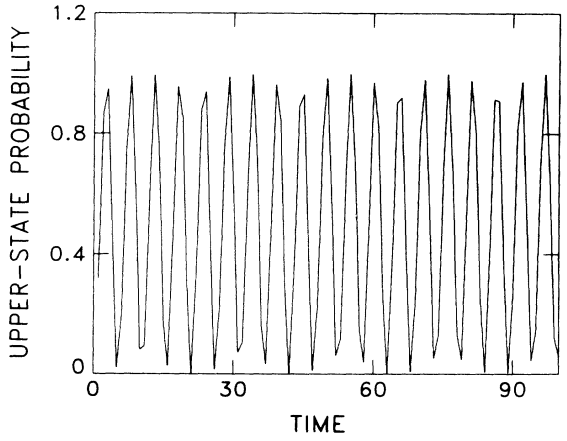

FIG. 1. Solution of (2.6) for the upper-state probability $|c_2(k)|^2$ for the case $\omega_0T=2\pi$, $\Omega T=0.60$, and $c_1(0)=1.0$.

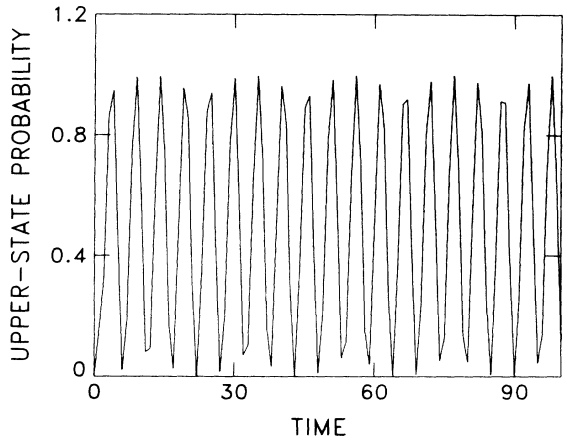

FIG. 2. Solution of the Bloch equations for the upper-state probability for the case $\omega=\omega_0$, $\bar{\Omega}T=1.2$.

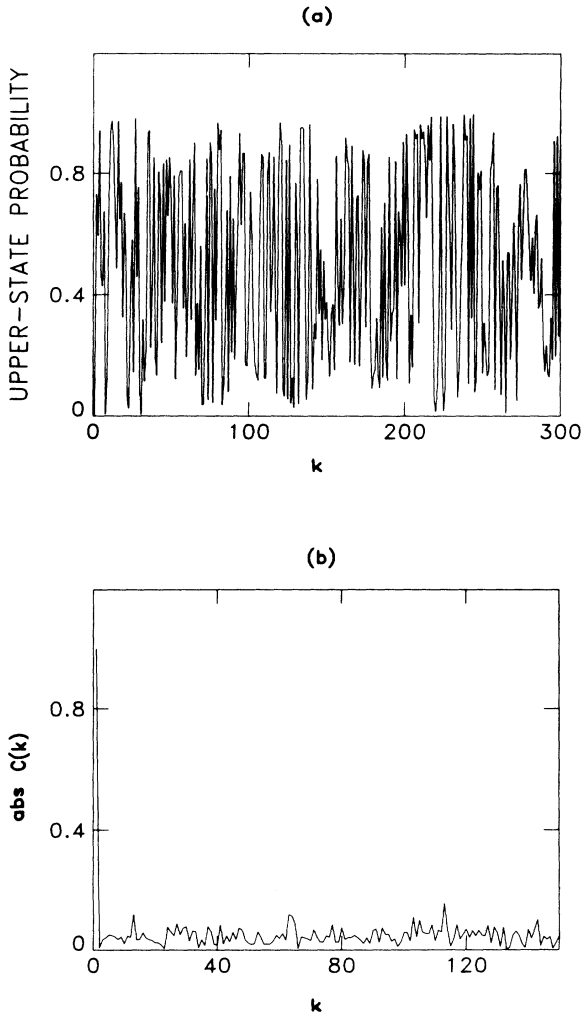

FIG. 3. (a) Upper-state probability and (b) absolute value of the autocorrelation function $C(\tau)$ for $\Omega T=500$, $\omega_0T=3.0$, x irrational.

In Fig. 2 we show the solution of the Bloch equations (2.7) for the upper-state probability $(1+z)/2$, assuming $\omega=\omega_0$ (i.e., $\omega_0 T=2\pi$) and $\bar{\Omega}T=1.2$. The solution is quite complicated but we plot only the values at times $t=nT$ in order to compare with the results of the discrete mapping. It is seen, as expected, that the mapping provides an excellent approximation to the solution of the Bloch differential equations (2.7). The agreement is best for small values of ΩT, where the effects of all the overtone frequencies implicit in the discrete mapping are small. For small ΩT the mapping is also accurate considerably far off resonance. It might be noted that for two-state atoms in optical fields the Rabi frequencies are very small compared with ω, i.e., $\Omega T \ll 1$.

It is useful to consider the autocorrelation function of the state vector, defined as

$$C(\tau)=\lim_{T\to\infty}(1/T)\int_0^T dt\langle\Psi(t)\,|\,\Psi(t+\tau)\rangle\ . \tag{2.9}$$

For the kicked two-state atom we consider

$$|C(k)|=\lim_{N\to\infty}(1/N)\left|\sum_{n=0}^{N} c_1^*(n)c_1(n+k)+c_2^*(n)c_2(n+k)e^{-ik\omega_0 T}\right| . \tag{2.10}$$

One of the characteristics of chaos is a rapid decay of correlations. We have computed the autocorrelation function (2.10) for the periodically kicked two-state system for a range of values of $\omega_0 T$ and ΩT, and have found that $C(k)$ is nondecaying. That is, there is no evidence of chaotic behavior for the periodically kicked two-state atom.

However, we find that $C(k)$ can decay rapidly in the case of a quasiperiodically kicked two-state system. Consider, for instance, the kicking with $F(t)=\cos(\omega' t)$, in which case

$$\Omega(k)=\Omega\cos(\omega' kT)=\Omega\cos(2\pi k\omega'/\omega)=\Omega\cos(2\pi kx)\ , \tag{2.11}$$

where x is the ratio of the two driving frequencies. A rational value of x means the two frequencies are commensurate. In such cases we obtain nondecaying autocorrelations. When x is irrational, however, the autocorrelations are found to decay rapidly for large values of ΩT. The correlations do not go exactly to zero; there are small but finite correlations even for large values of τ, as well as occasional peaks as high as around 0.4 in $|C(\tau)|$. But the behavior of the autocorrelation function is dramatically different from the case of rational x. In Fig. 3 we plot $|c_2(k)|^2$ and $|C(k)|$ for $\Omega T=500$ and an irrational value of x.[5] The decay of $C(k)$ certainly suggests chaotic time evolution of the state vector, and, moreover, the power spectrum of the time series of Fig. 3(a) is broadband (Fig. 4). These indications of quantum chaos are consistent with the conclusions of Pomeau *et al.*,[3] who integrated the Bloch differential equations for a bichromatic driving field and found decaying correlations and broadband spectra.

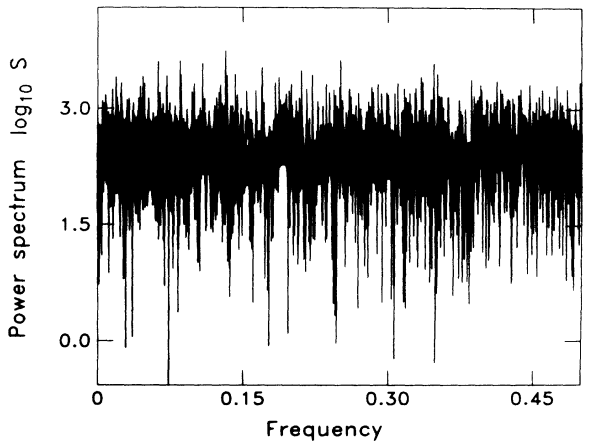

FIG. 4. Power spectrum of the upper-state probability amplitude.

It is convenient to define the three real Bloch variables

$$x(k)=a_1(k)a_2^*(k)+a_1^*(k)a_2(k)\ , \tag{2.12a}$$

$$y(k)=i[a_1^*(k)a_2(k)-a_1(k)a_2^*(k)]\ , \tag{2.12b}$$

$$z(k)=|a_2(k)|^2-|a_1(k)|^2\ , \tag{2.12c}$$

in terms of which the mapping (2.6) takes the form

$$x(k+1)=x(k)\cos(\omega_0 T)-y(k)\sin(\omega_0 T)\cos[2\Omega(k)T]-z(k)\sin(\omega_0 T)\sin[2\Omega(k)T]\ , \tag{2.13a}$$

$$y(k+1)=x(k)\sin(\omega_0 T)+y(k)\cos(\omega_0 T)\cos[2\Omega(k)T]+z(k)\cos(\omega_0 T)\sin[2\Omega(k)T]\ , \tag{2.13b}$$

$$z(k+1)=z(k)\cos[2\Omega(k)T]-y(k)\sin[2\Omega(k)T]\ . \tag{2.13c}$$

In the limit $T\to 0$ we recover the Bloch equations (2.7). Since the motion is confined to the Bloch sphere $x^2(k)+y^2(k)+z^2(k)=1$, (2.13) is also a mapping relating azimuthal and polar angles from kick to kick. The form (2.13) is useful for computing the surface of section (Poincaré map) of points $x(k),y(k)$ such that $z(k+1)=0$ and $z(k)>0$.[6] This provides a mapping on a circle, i.e., a mapping on the equator of the Bloch sphere.

In Fig. 5 we show this surface of section for the case of Fig. 3. The points appear to fill in the entire circle in an erratic sequence. A similar result is obtained for the surface of section in the xz plane. The surface of section in the yz plane fills only the semicircle $y^2+z^2=1$, $y>0$. This is a simple consequence of the Bloch equations: $\dot{x}<0$ implies $y>0$. In other words, the projection in the xy plane of trajectories on the Bloch sphere must always spiral in a counterclockwise sense.

These results for surfaces of section, which appear to be independent of the initial conditions on the probability amplitudes, suggest that trajectories on the Bloch sphere can cover the whole sphere when the kicking is done quasiperiodically. That is, in addition to decaying autocorrelations and broadband spectra, we appear to have ergodic motion on the Bloch sphere.

For an intuitive explanation of the origin of this "chaotic" behavior, consider the factors $\cos[\Omega(k)T] = \cos[\Omega T \cos(2\pi kx)]$ and $\sin[\Omega T \cos(2\pi kx)]$ appearing in the Schrödinger equation (2.6). For large values of ΩT, and irrational values of x, these functions vary erratically with k. We plot $\cos[\Omega T \cos(2\pi kx)]$ in Fig. 6, together with its autocorrelation function, for the case of Figs. 3 and 5. Note the rapid decay of the autocorrelation function, which does not occur at smaller values of ΩT, nor at rational values of x (Fig. 7). For large ΩT and irrational x, therefore, the probability amplitudes are being driven erratically and they evolve "chaotically."

We can summarize our results for the quasiperiodically kicked two-state system as follows. For commensurate driving frequencies the time evolution is regular, in the sense that the state vector remains correlated in time and the motion is nonergodic. For incommensurate driving frequencies and large Rabi frequencies, however, the time evolution is chaotic, in the sense that (a) the autocorrelation function of the state vector decays; (b) the power spectrum of the state vector is broadband; and (c) the motion of the state vector on the Bloch sphere is ergodic.

The properties (a)—(c) are reasonable criteria for "quantum chaos" of externally driven systems, in that they also characterize classical chaotic behavior. In the classical context, of course, there is an unambiguous definition of chaos, i.e., a system is chaotic if it has a positive Lyapunov exponent, implying very sensitive dependence on initial conditions. This hallmark of classical chaos is not shared by bounded quantum systems: A perturbation of the state vector cannot grow exponentially. In the absence of some quantity that one can compute to determine unambiguously whether a quantum system is "chaotic," there have been considerable differences of opinion not only about how quantum chaos should be defined, but also about whether there can even be such a thing as quantum chaos. We return briefly to these questions in Sec. IV.

Casati *et al.*[7] have recently discussed the dynamical sta-

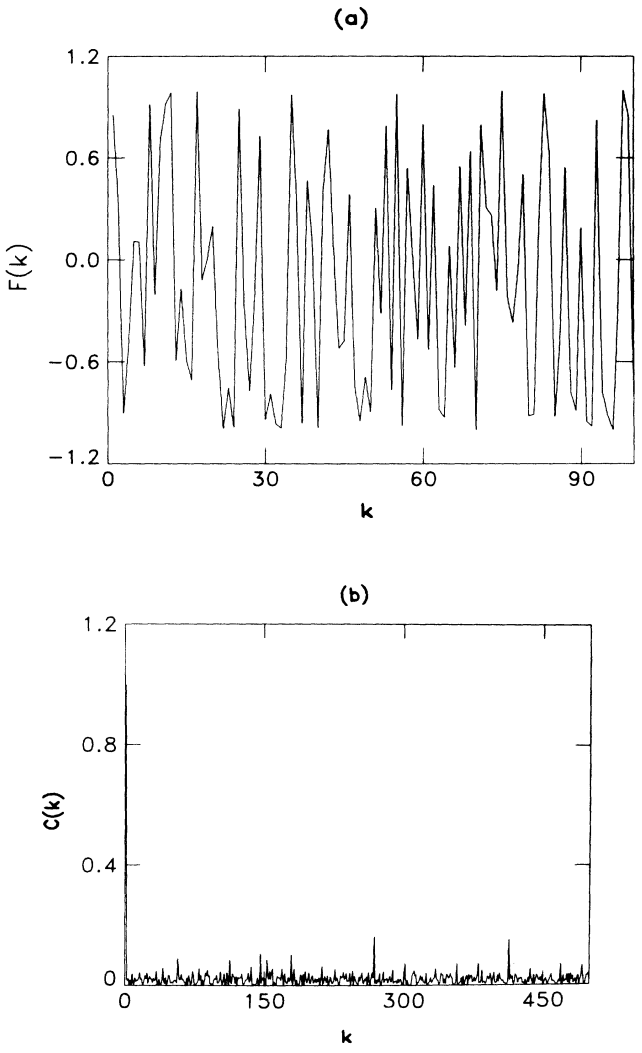

FIG. 6. (a) The function $\cos[\Omega T \cos(2\pi kx)]$ and (b) its autocorrelation function for the case of Fig. 3.

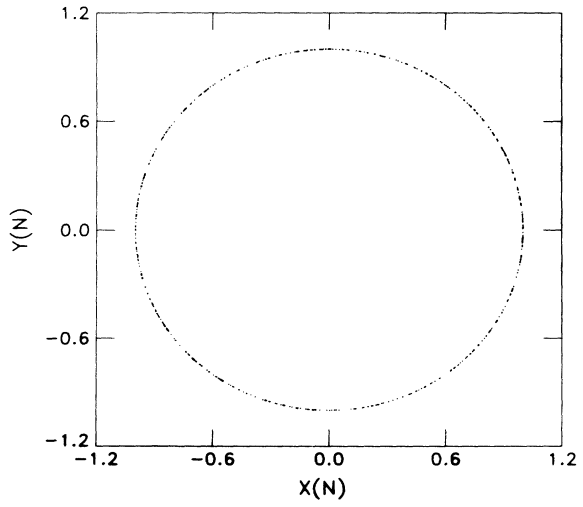

FIG. 5. Surface of section in the xy plane for the case of Fig. 3.

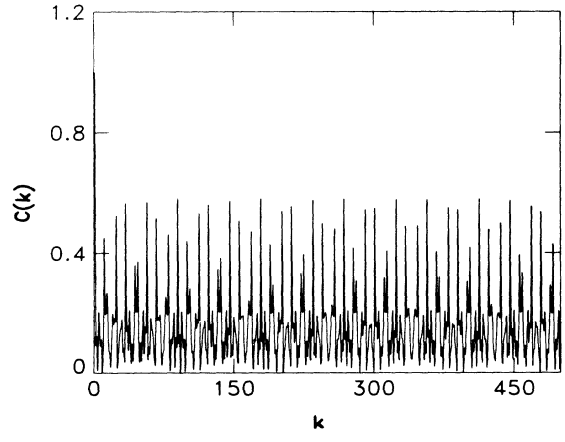

FIG. 7. Same as Fig. 6(b), except now $\Omega T = 10$.

bility of quantum "chaotic" behavior in the hydrogen atom driven by a monochromatic field. In a classically chaotic system the memory of the initial state is eventually lost due to the exponential instability implied by a positive Lyapunov exponent. In numerical experiments this means that backward integration does not reproduce the initial state for the forward integration. We have confirmed numerically that the backward mapping for the kicked two-state system does reproduce the initial state, thus providing another example of the greater degree of dynamical stability enjoyed by quantum systems.

III. THE KICKED PENDULUM

The results of Sec. II, suggest a reexamination of the kicked quantum rotator for the case in which the kicking is quasiperiodic. For the rotator $H_0=P_\theta^2/2ml^2$ and $E_n=n^2\hbar^2/2ml^2$. The unperturbed eigenfunctions of H_0 are $\psi_n(\theta)=(2\pi)^{-1/2}e^{in\theta}$, and so for $F(t)$ again taken to be $\cos(\omega' t)$ we have

$$V_{nm}(k)=(2\pi)^{-1}e^{-in^2/\tau/2} \times \int_0^{2\pi} d\theta\, e^{i(m-n)\theta} e^{-iA(\theta)T\cos(2\pi kx)/\hbar}, \quad (3.1)$$

where $\tau=\hbar T/ml^2$. Taking $A(\theta)=-(ml^2\omega_0^2)\cos\theta$, we obtain

$$\begin{aligned} V_{nm}(k)&=(2\pi)^{-1}e^{-in^2\tau/2}\int_0^{2\pi} d\theta\, e^{i(m-n)\theta}e^{iK(k)\cos\theta} \\ &=(2\pi)^{-1}e^{-in^2\tau/2}\int_0^{2\pi} d\theta\, e^{i(m-n)\theta} \\ &\quad\times\sum_{s=-\infty}^{\infty} b_s[K(k)]e^{is\theta} \\ &=b_{n-m}[K(k)]e^{-in^2\tau/2}, \end{aligned} \quad (3.2)$$

where

$$K(k)=(ml^2\omega_0^2T/\hbar)\cos(2\pi kx)=K\cos(2\pi kx) \quad (3.3a)$$

and

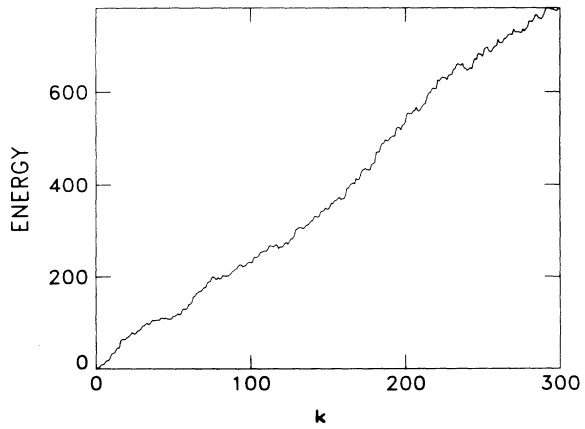

FIG. 8. Plot of the energy (3.5) for the quantum rotator with $K=10$, $\tau=1$, and x irrational.

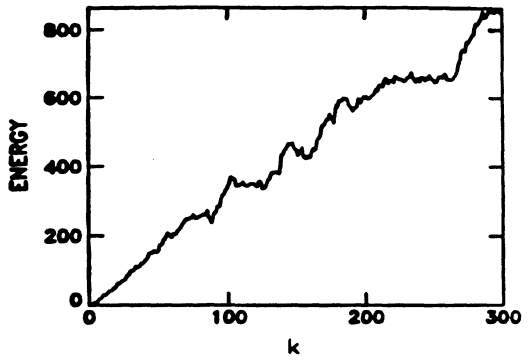

FIG. 9. Classical result corresponding to Fig. 8.

$$b_s(y)=i^sJ_s(y), \quad (3.3b)$$

with J_s the Bessel function of the first kind of order s. The Schrödinger equation (2.4) then becomes

$$c_n(k+1)=\sum_m b_{n-m}[K(k)]e^{-in^2\tau/2}c_m(k), \quad (3.4)$$

where $c_n(k)=a_n(k)e^{in^2\tau/2}$. When $F(t)=1$, $x\to 0$ and equation (3.4) reduces to the equation solved numerically by Casati *et al.*[1]

For x rational we obtain the "localization" behavior noted earlier. With x irrational, however, it appears we can have the diffusive energy growth predicted by the (periodically kicked) classical model. In Fig. 8 we plot the energy (in units of $m\omega_0^2l^2/2$)

$$\langle E(k)\rangle=\tau K^{-1}\sum_{-N}^{N} n^2|c_n(k)|^2, \quad (3.5)$$

where N is a large integer, typically ≈ 400, chosen large enough that the total probability is conserved at each iteration. For Fig. 8 we chose $K=10$, $\tau=1$, and $x=4637/13\,313$, which for practical purposes is an irrational,[5] and the rotator is assumed to be in the ground state at $t=0$. After 300 iterations there is no evidence of any quantum suppression of the classical diffusion. For comparison we show in Fig. 9 the corresponding classical results obtained from the standard map[1] modified for the case of quasiperiodic kicking:

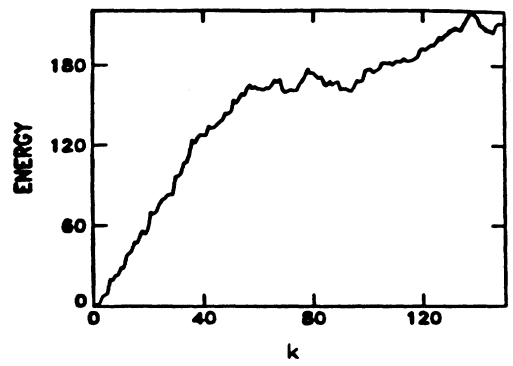

FIG. 10. Energy (3.5) for the quantum rotator with $K=10$, $x=\frac{1}{3}$.

$$P_{k+1}=P_k-\bar{K}(k)\sin\theta_k\ , \tag{3.6a}$$

$$\theta_{k+1}=\theta_k+P_{k+1}\ , \tag{3.6b}$$

with $\bar{K}(k)=\bar{K}\cos(2\pi kx)$, $\bar{K}=K\tau=10$. Figure 9 was obtained by averaging over results for a set of 40 initial angles θ_0. In Fig. 10 we show the results for the quantum rotator with $K=10$ and $x=\frac{1}{3}$. In this case there is significant suppression of the classical energy growth after ≈ 60 kicks.

Shepelyansky[8] has also found that two-frequency kicking can greatly extend the time scale over which diffusive energy growth occurs in the kicked quantum rotator, and has suggested that the diffusive time scale in this case increases exponentially with K. It is perhaps worth noting that the addition of more kicking frequencies effectively increases the dimensionality of the system. Since Anderson localization is most effective in one dimension, it is to be expected that the addition of more driving frequencies acts to weaken the quantum localization effect.

IV. REMARKS

Our main criterion for quantum chaos of these kicked systems has been the decay of the autocorrelation function of the state vector. Since this autocorrelation function is related by Fourier transformation to the power spectrum this decay implies that the power spectrum does not consist solely of δ-function peaks, as in the case of quasiperiodic motion. We suspect that such quantum chaos is not unusual in quasiperiodically driven systems.

This criterion appears to us to be a reasonable one. It has also been used by Pomeau, Dorizzi, and Grammaticos[3] and, in the time-independent domain for a single energy eigenstate, by Shapiro and Goelman.[9] Of course, it is widely recognized that quantum chaos cannot entail the same degree of dynamical instability, in the sense of a positive Lyapunov exponent, as classical chaos. In the quasiperiodically kicked two-state system, for instance, we have confirmed that the chaotic time evolution is fully reversible, not only in principle but in practical computations.[7] That is, the quantum dynamics smooths out the classical instability associated with very sensitive dependence on initial conditions. This smoothing effect is perhaps best understood in terms of the summing over classical paths that is implicit in the quantum dynamics; we hope to discuss this point in a future publication.

ACKNOWLEDGMENT

This work was supported in part by National Science Foundation Grant No. PHY-8418070 at the University of Arkansas.

[1]G. Casati, B. V. Chirikov, J. Ford, and F. M. Izrailev, *Stochastic Behavior in Classical and Quantum Hamiltonian Systems,* Vol. 93 of *Lecture Notes in Physics,* edited by G. Casati and J. Ford (Springer, Berlin, 1979).

[2]D. R. Grempel, R. E. Prange, and S. Fishman, Phys. Rev. A **29**, 1639 (1984).

[3]Y. Pomeau, B. Dorizzi, and B. Grammaticos, Phys. Rev. Lett. **56**, 681 (1986).

[4]See, for instance, L. Allen and J. H. Eberly, *Optical Resonance and Two-Level Atoms* (Wiley, New York, 1975).

[5]For numerical computations we can take x to be the ratio of two large primes. Following Pomeau *et al.* (Ref. 3) we present here results for $x=4637/13\,313$ as our "irrational."

[6]For the discrete mapping we define the surface of section in the xy plane by $|z(k)|<0.01$ and $z(k)<z(k-1)$.

[7]G. Casati, B. V. Chirikov, I. Guarneri, and D. L. Shepelyansky, Phys. Rev. Lett. **56**, 2437 (1986).

[8]D. L. Shepelyansky, Physica D **8**, 208 (1983).

[9]M. Shapiro and G. Goelman, Phys. Rev. Lett. **53**, 1714 (1984).